

SLAB FRACTURE AT 1900 FRAMES PER SECOND—EXPERIMENTAL METHODS

Chris Borstad\*, David McClung  
University of British Columbia

**ABSTRACT:** We present high speed video images of slab fracture experiments. Slab bending tests were conducted in a cold laboratory at Rogers Pass in Glacier National Park of Canada. A testing machine recorded the applied force and slab deflection in three- and four-point bending. Over the course of four days, the bending and resulting tensile fracture of 66 samples were captured by a high speed camera at rates of 1000 and 1900 frames per second. The purpose of capturing the tests on video was to observe the size of the fracture process zone and to calculate the speed of crack propagation. Slab samples were seeded with tracer particles for image analysis calculations, with the resulting pixel resolution in the sub-millimeter range. The samples were back-lit to illuminate the propagation of the crack. Dry slabs of differing density, hardness, crystal form and size, and temperature were sampled. Slabs of the same composition but different size were tested to investigate the size effect. The peak strength, stiffness, and shape of the loading curve were found to be very sensitive to the loading rate.

**KEYWORDS:** fracture mechanics, high speed photography

## 1. INTRODUCTION

The purpose of this research was to record slab fracture at a rate and scale appropriate to observe several important details of the fracture. First, observation of the straining of the sample, both prior to fracture and ahead of a developing and propagating fracture, tests our existing notions about the size of the fracture process zone (FPZ). The FPZ size is a very important material property in the fracture mechanics of snow. Previous estimates or calculations of this property have been measured or inferred indirectly or theoretically calculated rather than directly observed.

Second, the speed of crack propagation can be calculated accurately using a high speed camera. This is important because the speed of a crack relative to the appropriate wave speed of a material determines whether dynamic or static fracture mechanics must be used to model the fracture.

Finally, detailed high speed images of the experiments allow analysis of the testing apparatus and its coupling with the snow sample. Crushing of the sample at the supports or at the point of load application can be measured. Any spring-back of the loading apparatus or load cell can be detected, which is important when measuring the strain-softening displacement. The video images also allow confirmation that displacement sensors are working and properly mated to the sample.

This paper outlines the experimental methods used in this project. A full paper including analysis and results is planned for a future publication.

## 2. METHODS

### *2.1 Cold Laboratory*

The experiments were carried out in a cold laboratory located at Rogers Pass in Glacier National Park of Canada. The temperature of the lab can be controlled down to about  $-20^{\circ}\text{C}$ . The lab was always kept colder than about  $-5^{\circ}\text{C}$  to avoid any melting of the sample during preparation or handling, as some instruments melted snow crystals at higher temperatures. Minor fluctuations in temperature occur during occasional defrost cycles and when the lab door is opened. Humidity control is unavailable in the lab.

The air in the lab is dry compared to the vapour-saturated interstitial air in the snowpack. For this reason, snow samples are tested as soon as possible after extraction and transportation to the lab. Typically a short amount of time is allowed for all of the snow samples to equilibrate with the temperature of the lab. However, the relative humidity difference between the remaining interstitial air in the snow sample and that of the lab leads to a vapour flux out of the snow sample. The result is a metamorphism of the snow sample crystals.

By setting the temperature of the laboratory equal to the temperature of the snowpack where the samples were extracted, the rate of metamorphism of the samples is minimized. The relative humidity difference is unavoidable, however. For this reason the tests were all carried out on the same day as the samples were extracted. This ensures that the snow crystals and bonding structure are as close as possible to those in the snowpack. Previous overnight storage of samples led to an observable change in the samples from their original state.

---

\* *Corresponding author address:* Chris Borstad,  
Department of Civil Engineering, University of British  
Columbia, 1984 West Mall, Vancouver, BC V6T 1Z2;  
email: cborstad@civil.ubc.ca

## 2.2 Study Plot and Sample Collection

For this series of experiments, the samples were obtained from a study plot near the laboratory in a sheltered location at an elevation of 1330 m. A standard snow profile observation was conducted first, following Canadian Avalanche Association standards (Canadian Avalanche Association, 2007). The observation wall of the snow pit was then extended to provide the necessary room to extract the samples. It was typically possible to extract and test 15-20 samples in a day. Samples were carried directly from the study plot to the laboratory on foot. Figure 1 shows a picture of a snow pit after the profile and sample extraction were carried out.



Figure 1: Photograph of a snow pit after a standard profile observation and extraction of samples. Samples of different sizes were taken from a slab layer that extends from the lower right corner of the picture.

The samples were excised using stainless steel rectangular boxes, open on both ends—similar to an air duct. Three different sample/cutter sizes were used: 10 cm x 5 cm x 20 cm; 10 cm x 10 cm x 40 cm; 10 cm x 20 cm x 80 cm. The slope-normal dimension of the samples was always 10 cm, with the two longer dimensions within the slab layer. Homogeneous slab layers at least 10 cm thick were targeted in order to minimize the number of variables being tested.

Figure 2 shows a schematic of the orientation and relative sizes of the samples. Schwiezer et. al. (2004) reported that for mode I (tensile) fractures in field tests, the variation in test results was substantially reduced by orienting the fracture in a similar manner. The alternative would be to orient the samples as in Figure 3. In this orientation, however, it is very difficult to find homogeneous samples. Slab layers that are 20

cm-thick without an appreciable gradient in properties with depth are rare. Even 10 cm layers can be difficult to find at times over the course of a winter.

Most of the snow samples used in this series were composed of small, rounded crystals, 0.5-1 mm in size, in the pencil hardness range. The density of samples ranged from about 245-330 kg/m<sup>3</sup>.

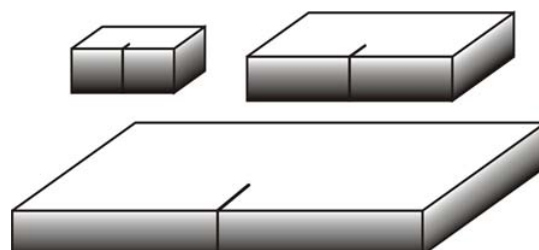


Figure 2: Relative size and orientation of snow samples. The samples are fractured in bending such that a tensile fracture travels in the direction of the notch across the sample.

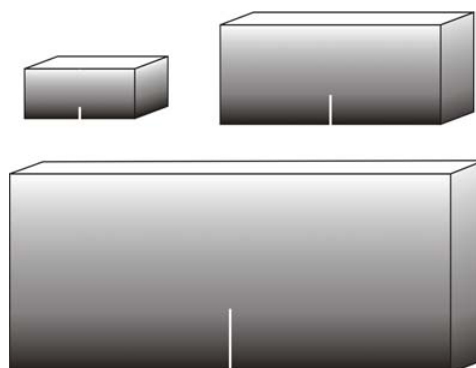


Figure 3: Alternative vertical orientation of slab samples. In this case the fracture would travel upward through the slab and across layers. Higher variability of results would be expected.

## 2.3 Testing Methods

A ball-screw driven, computer controlled bench-top testing machine supplied by Adelaide Testing Machines was used for the experiments. The machine was outfitted with an adjustable three or four point bending apparatus. This testing orientation creates a propagating tensile fracture on the tensile face of the bending specimen (Figure 4).

The computer controlling the testing machine records the applied force  $P$  through a load cell with a capacity of 250 N. The sampling frequency of the applied force is adjustable, and was typically set in the neighbourhood of 1000 Hz. The load-point deflection was also monitored at the same frequency. Two external linear variable differential transformers (LVDTs) were attached to the sample to monitor

deflection at different points, typically the bottom of the sample where the fracture originates and on the top of the sample opposite one of the support plates.

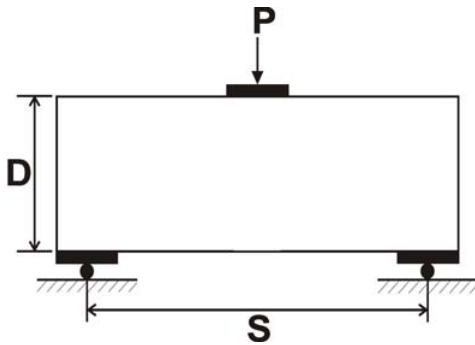


Figure 4: Schematic of a three-point-bending test specimen. A tensile fracture originates on the face opposite the applied force  $P$ , and propagates across the sample. The span to depth ratio  $S/D$  was kept constant for samples of varying volume.

The high speed camera used to film the tests was a Phantom v4.2 from Vision Research. Camera control and data acquisition was by an external laptop. The camera was mounted to a tripod and zoomed in on the sample as much as the lens would allow without losing focus. The camera body was completely insulated with styrofoam to protect it against the cold temperature.

The camera was capable of filming as fast as 1900 frames per second. At this rate it could record for about 2 seconds. At the fastest loading rates possible for the testing machine, a typical test lasted a

fraction of a second. At slow loading rates, however, a test can last on the order of a second. In these cases the camera capture rate was set at 1000 frames per second to ensure that the entire test was recorded.

The snow samples were seeded with black peppercorns on a 2 cm grid. This was to provide contrast for the film and to allow post-processing of the video images by particle tracking software. The samples were also back-lit by a lamp to illuminate the crack as it propagates.

The video images were saved on an external drive, with each test file composed of thousands of individual images. A typical test file was on the order of several gigabytes in size and took around 5 minutes to save.

#### ACKNOWLEDGEMENTS

We would like to thank Canadian Mountain Holidays and the Natural Sciences and Engineering Research Council of Canada for supporting this research.

#### REFERENCES

- Canadian Avalanche Association, 2007. Observation Guidelines and Recording Standards for Weather, Snowpack and Avalanches. A revision of NRCC Technical Memorandum No. 132, Revelstoke, B.C., 90 pp.
- Schweizer, J., Michot, G., Kirchner, H.O.K., 2004. On the fracture toughness of snow. *Ann. Glaciol.* 38 (1), 1-8.